

# Meyer–Neldel rule for dark current in charge-coupled devices

Ralf Widenhorn, Lars Mündermann,<sup>a)</sup> Armin Rest,<sup>b)</sup> and Erik Bodegom<sup>c)</sup>

*Department of Physics, Portland State University, Portland, Oregon 97207*

(Received 11 January 2001; accepted for publication 22 March 2001)

We present the results of a systematic study of the dark current in each pixel of a charged-coupled device chip. It was found that the Arrhenius plot, at temperatures between 222 and 291 K, deviated from a linear behavior in the form of continuous bending. However, as a first approximation, the dark current,  $D$ , can be expressed as:  $D = D_0 \exp(-\Delta E/kT)$ , where  $\Delta E$  is the activation energy,  $k$  is Boltzmann's constant, and  $T$  the absolute temperature. It was found that  $\Delta E$  and the exponential prefactor  $D_0$  follow the Meyer–Neldel rule (MNR) for all of the more than 222,000 investigated pixels. The isokinetic temperature,  $T_0$ , for the process was found as 294 K. However, measurements at 313 K did not show the predicted inversion in the dark current. It was found that the dark current for different pixels merged at temperatures higher than  $T_0$ . A model is presented which explains the nonlinearity and the merging of the dark current for different pixels with increasing temperature. Possible implications of this finding regarding the MNR are discussed. © 2001 American Institute of Physics. [DOI: 10.1063/1.1372365]

## I. INTRODUCTION

The Meyer–Neldel rule (MNR) is an empirical law known since 1937.<sup>1</sup> It relates the activation energies,  $\Delta E$ , and the exponential prefactors,  $X_0$ , for processes that obey the equation

$$X = X_0 \exp(-\Delta E/kT). \quad (1)$$

The rule states that  $X_0$  as a function of  $\Delta E$  is given by

$$X_0 = X_{00} \exp(\Delta E/E_{MN}), \quad (2)$$

where  $X_{00}$  and  $E_{MN}$  are positive constants. The observed values for the characteristic energy,  $E_{MN}$ , in various different materials and processes, have been measured to be between 25 and 100 meV.

The hallmarks of the MNR, linear behavior of the Arrhenius plot and a characteristic temperature where the compensation is exact, are often recognized. Especially the conductivity for various semiconductors shows Meyer–Neldel behavior, see for example Refs. 2–4. The rule is generally observed in disordered materials. Even though a number of theoretical models to explain the origin of the MNR are proposed, none of them is universally accepted. Some argue the MNR arises because of an exponential density of states (DOS) distribution that induces a shift in the Fermi level.<sup>5</sup> This DOS has been found in inorganic amorphous semiconductors, but the MNR is more generally applicable.<sup>6</sup> Furthermore, this model results in prefactors for the conductivity, which are difficult to interpret physically.<sup>7</sup> Jackson<sup>8</sup> explains the MNR for nonequilibrium time-dependent processes by multitrapping over a fixed distance. Others argue that the rule arises from the entropy of combining multiple

excitations.<sup>7,9,10</sup> In various experiments, the MNR is found even if the experimental data shows deviations from the Arrhenius law.<sup>11–17</sup>

The dark count in a Charge-Coupled Device (CCD) gives a unique possibility (more than 222,000 samples can be used to verify the MNR) to investigate the MNR and its underlying mechanism. We investigated the dark count primarily at temperatures between 222 and 291 K and found that the dark count in some pixels increases more than five orders of magnitude. If approximated by Eq. (1), the dark count follows the MNR [Eq. (2)] remarkably well. The characteristic energy,  $E_{MN}$ , was determined to 25.3 meV. Finally, we will discuss the case when the temperature approaches and exceeds  $T_0$ .

## II. EXPERIMENT

The research presented here will focus on the dark current in a CCD camera. The heart of the camera, the CCD chip, is composed of an array of metal oxide semiconductor capacitors (the pixels). CCDs detect light by collecting electrons, which are excited by the photoelectric effect from the valence band into the conduction band of a doped semiconductor. An external applied field collects the excited electrons separately for each pixel. The resulting electron distribution over the chip represents the picture. Even though the chip is not exposed to light, electrons are thermally excited into the conduction band. These electrons cause the so-called dark count. The dark count is not uniform for all pixels. Impurities enhance the dark current (i.e., the dark count per second) significantly. They are also responsible for other unwanted effects, like residual images.<sup>18,19</sup> The dark count becomes more important for low-light level imaging with long integration times. Astronomers correct their images by subtracting a calibrated “dark frame” from their image. A dark frame can be obtained by taking a picture without opening the shutter, i.e., without exposing the chip to light. We in-

<sup>a)</sup>Also at: Department of Computer Science, University of Calgary, Calgary, Alberta, Canada T2N 1N4.

<sup>b)</sup>Also at: Astronomy Department, University of Washington, Seattle, Washington 98195.

<sup>c)</sup>Electronic mail: bodegom@pdx.edu

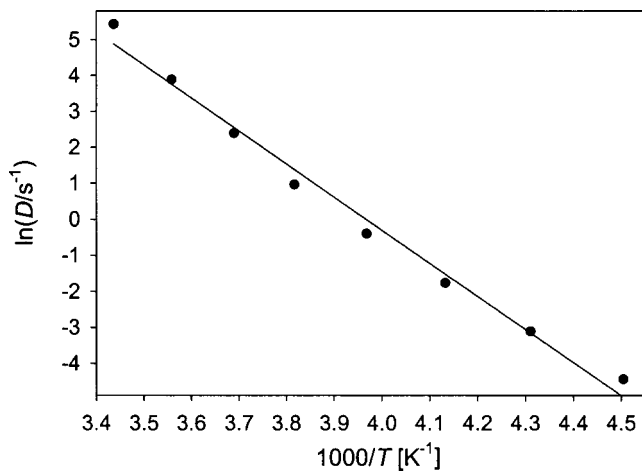


FIG. 1. Average of the logarithm of the dark current vs the inverse temperature and the best linear fit through the data points.

investigated the dark count for an array of  $472 \times 472$  pixel subframe and could, therefore, study the temperature dependence of the dark current and the MNR for more than 222,000 samples.

The backside-illuminated chip ( $12.3 \text{ mm} \times 12.3 \text{ mm}$ ,  $512 \times 512$  pixels, manufactured by SITE Inc.) with an individual pixel size of  $24 \mu\text{m} \times 24 \mu\text{m}$  was housed in a SpectraVideo camera (Model: SV512V1, manufactured by Pixelvision, Inc.). The chip was a three phase,  $n$ -buried channel, three-level polysilicon back-thinned device. The chip used in this study showed a linear dark count versus exposure time dependence for all pixels. Thus, the dark current at a particular chip temperature could be determined by fitting the counts linearly versus the exposure time. In order to minimize uncertainties due to the readout noise, the dark counts were calculated as the average of several images. 50 pictures were taken for each of the following exposure times: 3, 5, 10, 20, 50, and 100 s and 20 images each for 250 and 500 s and finally ten pictures at 1000 s. The camera was equipped with a double-stage, water-cooled, thermoelectric cooling system that allowed us to operate the chip at temperatures as low as 222 K. The dark currents at 222, 232, 242, 252, and 262 K were calculated based on the pictures taken between 3 and 1000 s. The number of thermally released electrons into the conduction band increases with increasing temperatures, and some pixels at temperatures higher than 262 K were saturated for longer exposure times. Therefore, the dark current at 271 K was based on the frames taken between 3 and 500 s, at 281 K between 3 and 250 s, and at 291 K, between 3 and 50 s, respectively.

### III. RESULTS AND DISCUSSION

The Arrhenius plot for the average dark current (average for all 222,784 pixels) is displayed in Fig. 1. Each of the data points contains information of at least 55 million (at 293 K) and up to 77 million (at 222–262 K) measurements (the number of the pictures taken at a given temperature times 222,784 for the  $472 \times 472$  subframe).

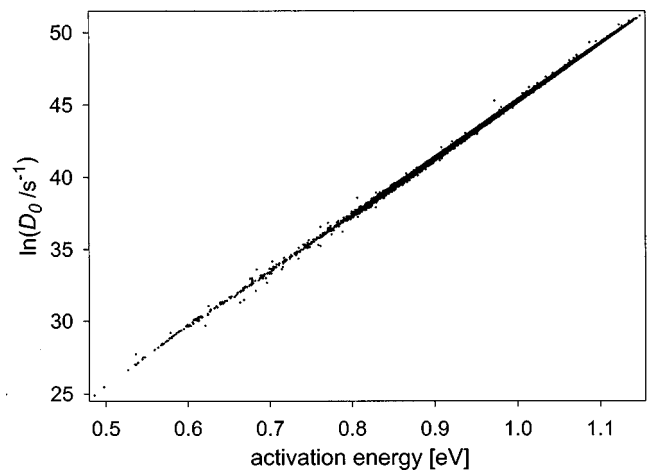


FIG. 2. Correlation between  $\ln(D_0)$  and  $\Delta E$  for dark current in a CCD camera.

As a first approach, the nonlinearity in the Arrhenius plot was neglected. Thus, in this approximation, the dark current can be written as:

$$D = D_0 \exp(-\Delta E/kT) \quad (3)$$

Similarly, we fitted Eq. (3) to the data for each of the 222,784 individual pixels. We thus obtained 222,784 pairs of activation energies and exponential prefactors. The average activation energy was calculated to 1 eV. This roughly corresponds to the band gap in silicon. Impurity states between the bands facilitate electrons to reach the conduction band and decrease the effective activation energy. Unequal distribution of impurities causes a spread in the values for the activation energy. Figure 2 shows the correlation between the fitted values for  $\Delta E$  and  $\ln(D_0)$  for the 222,784 individual pixels. The linear relation, predicted by the MNR [Eq. (2)], is remarkably precise for all data points. The characteristic energy was determined to be  $E_{MN} = 25.3 \text{ meV}$  and  $D_0$ , which is equal to the theoretical dark current at  $T_0$  was given by  $312 \text{ s}^{-1}$ .

The dark current expressed with the two Meyer–Neldel constants (i.e., by substituting Eq. (2) into Eq. (1)) is given by:

$$D = D_{00} \exp\left(\left[\frac{1}{E_{MN}} - \frac{1}{kT}\right] \Delta E\right). \quad (4)$$

At  $T_0 = E_{MN}/k = 294 \text{ K}$ , one would expect the dark current to be independent of  $\Delta E$ . Thus, at this temperature, all pixels should show the same dark current. Figure 3 shows the Arrhenius plot for four random pixels. The values for  $\ln(D)$  at low temperatures differ significantly, but they come closer with increasing temperatures. Finally, in good agreement with the MNR, the curves almost coincide at 291 K.

At temperatures higher than  $T_0$ , the MNR predicts an inversion in the count rate.<sup>20–22</sup> Pixels with a dark current larger than average at temperatures less than  $T_0$ , should show a smaller than average value at temperatures larger than  $T_0$ . To explore this phenomenon, we heated the chip up to 313 K. At this temperature some, “hot” pixels (high dark current at low temperatures) indeed showed this inversion.

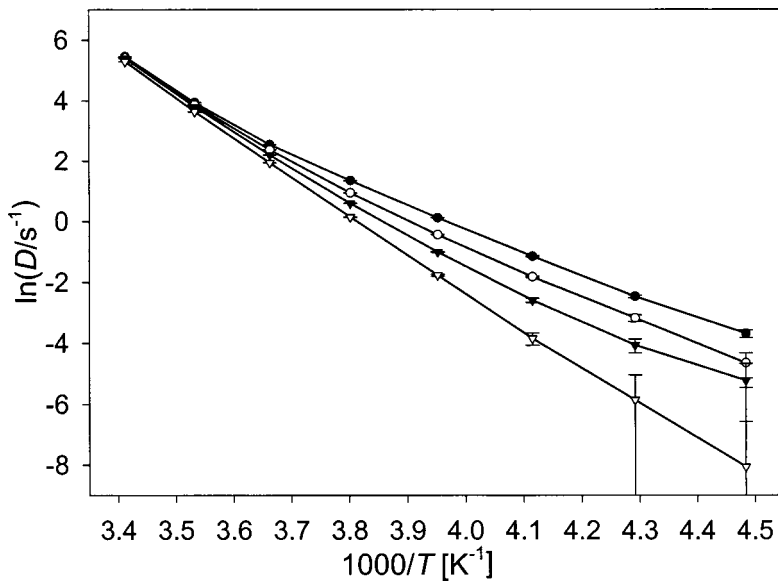


FIG. 3.  $\ln(D)$  vs the inverse temperature for four different pixels.

However, most hot pixels still displayed a slightly higher dark current. Thus, the inversion predicted by the Meyer–Neldel compensation law could not be observed.

The plot of  $\ln(D)$  versus the inverse temperature deviated from a linear line or Arrhenius behavior described by  $D = D_0 \exp(-\Delta E/kT)$  (see Figs. 1 and 3). The data points in the Arrhenius plot display a slightly positive curvature. Deviations from a linear behavior are often observed. It is quite likely that in other experiments the same effect could have been observed, had it not been for experimental uncertainties, the limited temperature range and the sparse data. The origin of this deviation may vary from experiment to experiment. Some found a linear dependence with  $T^{-1/4}$  at low temperatures and identified the transport mechanism as dominated by variable range hopping, which is described by Mott’s law.<sup>11,14,15</sup> At higher temperatures, Yoon *et al.*<sup>23</sup> argue that the statistical shift of the Fermi level can cause the observed bending. For our experiment, a calculation based on quantum mechanical considerations of the DOS and the probability of the occupation of these states can explain the bending in part. The number of electrons in the conduction band, as a function of the band gap energy and the temperature, can be derived for an intrinsic semiconductor.<sup>24</sup> This occupation probability is expressed by the Fermi function. Integration over the number of electrons with energy larger than the energy of the bottom of the conduction band results in a population of the conduction band that is proportional to  $T^{3/2} \exp(-\Delta E/kT)$ . However, this additional  $T^{3/2}$  term can not explain our data sufficiently. A model that fits our data better is similar to the one Herz *et al.*<sup>25</sup> proposes for the conductivity of a polycrystalline film. Multiple acceptor levels were introduced to explain the nonlinearity in the  $\ln(D)$  versus  $T^{-1}$  plot.

We assume that two distinct processes contribute to the dark current. One process dominates at low temperatures and the other is more important at higher temperatures. The average activation energies (over 222,784 pixels) for the two processes were determined to 0.61 and 1.18 eV for the low and high temperature regime, respectively (Fig. 4).

The two processes were identified as follows. At low temperatures, the energy available to electrons is too low for them to overcome the band gap directly and excitations involving impurities are dominant. The average activation energy of 0.61 eV corresponds well with this assumption and with other experiments in CCDs, where impurities with approximately the same energy levels were found (in particular Au, Ni, and Co).<sup>26,27</sup> With increasing temperatures, the intrinsic transition becomes dominant. At 313 K, the impurity process contributes only 2% to the dark current and the dark current becomes almost independent of the impurities. The superposition of both excitations results in a positive curvature in the Arrhenius plot.

Furthermore, this model explains the merging of the lines in the plot of  $\ln(D)$  versus the inverse temperature with increasing temperatures. A linear fit to these lines will display the intersection at  $T_0$ . The result for this intersection as well as the values for  $\Delta E$  is inseparably linked to the temperatures used for the fit.

$E_{MN}$  determines the temperature where the extrapolated Arrhenius plots would intersect.  $D_{00}$  is the dark current at this temperature. At temperatures higher than  $T_0$ , our model predicts that the dark current is determined by the band gap. Therefore, it should be the same for all pixels. The dark

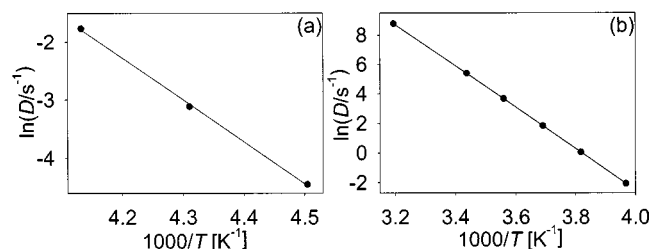


FIG. 4. (a) The logarithm of the average dark current (472×472 pixel) vs inverse temperature at 222, 232, and 242 K. (b) The logarithm of the residual dark current vs the inverse temperature from 252 to 313 K. The straight lines are the best linear fits through the data points.

current will only differ due to statistical uncertainties and the small influence of impurities.

To our knowledge, only Fortner *et al.*<sup>20,21</sup> could measure values where  $kT > E_{MN}$ . Nobody has measured the intercept at  $T_0$ . We think it is of fundamental importance for the understanding of the MNR to know if an actual inversion for a particular process can be found. Our results indicate that the MNR is only applicable in a small temperature range and does not apply for  $T$  approaching  $T_0$ .

#### IV. CONCLUSIONS

We showed that the CCD camera gives easy access to the verification of the MNR in a thermally activated process. Based on a linear fit for  $\ln(D)$  versus  $T^{-1}$ , the dark current obeys the MNR very well. We demonstrated that the Arrhenius plot showed deviations from the linear behavior in the form of a positive curvature. We have proposed a model that explains the bending in the Arrhenius plot, as well as the convergence of the dark current when the temperature approaches  $T_0$ . Since our assumptions are not specific to dark current, it is likely to be applicable to other processes as well. Finally, we think that further effort should be focused on verifying whether there is an inversion temperature. This would bring about a deeper understanding of the origin of the MNR.

#### ACKNOWLEDGMENTS

This work was partially supported by PixelVision of Oregon, Inc., Tigard, OR, and a Space Science Telescope Institute/NASA grant under the IDEA program.

- <sup>1</sup>W. Meyer and H. Neldel, Z. Tech. Phys. (Leipzig) **12**, 588 (1937).
- <sup>2</sup>Y. Lubianiker and I. Balberg, Phys. Rev. Lett. **78**, 2433 (1997).
- <sup>3</sup>K. Shimakawa and F. Abdel-Wahab, Appl. Phys. Lett. **70**, 652 (1996).
- <sup>4</sup>Y. F. Chen and S. F. Huang, Phys. Rev. B **44**, 13775 (1991).
- <sup>5</sup>H. Overhof and P. Thomas, *Electronic Transport in Hydrogenated Amorphous Semiconductors* (Springer, Berlin, 1989).
- <sup>6</sup>A. Yelon and B. Movaghar, Appl. Phys. Lett. **71**, 3549 (1997).
- <sup>7</sup>A. Yelon, B. Movaghar, and H. M. Branz, Phys. Rev. B **46**, 12244 (1992).
- <sup>8</sup>W. B. Jackson, Phys. Rev. B **38**, 3595 (1988).
- <sup>9</sup>G. Boisvert, L. J. Lewis, and A. Yelon, Phys. Rev. Lett. **75**, 469 (1995).
- <sup>10</sup>A. Yelon and B. Movaghar, Phys. Rev. Lett. **65**, 618 (1990).
- <sup>11</sup>D. H. Tassis, C. A. Dimitriadis, and O. Valassiades, J. Appl. Phys. **84**, 2960 (1998).
- <sup>12</sup>J. C. Wang and Y. K. Chen, Appl. Phys. Lett. **73**, 948 (1998).
- <sup>13</sup>K. Morii, T. Matsui, H. Tsuda, and H. Mabuchi, Appl. Phys. Lett. **77**, 2361 (2000).
- <sup>14</sup>C. Guillén and J. Herrero, J. Appl. Phys. **71**, 5479 (1992).
- <sup>15</sup>D. H. Tassis, C. A. Dimitriadis, J. Brini, G. Kamarinos, and A. Birbas, J. Appl. Phys. **85**, 4091 (1999).
- <sup>16</sup>E. J. Meijer, M. Matters, P. T. Herwig, D. M. de Leeuw, and T. M. Klapwijk, Appl. Phys. Lett. **76**, 3433 (2000).
- <sup>17</sup>P. A. W. E. Verleg and J. I. Dijkhuis, Phys. Rev. B **58**, 3917 (1998).
- <sup>18</sup>A. Rest, L. Mündermann, R. Widenhorn, T. McGlenn, E. Bodegom, *Residual Images in Charge-coupled Devices (to be published)*.
- <sup>19</sup>J. R. Janesick, T. Elliot, S. Collins, M. Blouke, J. Freeman, Opt. Eng. **26**, (1987).
- <sup>20</sup>J. Fortner, M.-L. Saboungi, and J. E. Enderby, Philos. Mag. Lett. **68**, 85 (1993).
- <sup>21</sup>J. Fortner, V. G. Karpov, and M.-L. Saboungi, Appl. Phys. Lett. **66**, 997 (1995).
- <sup>22</sup>I. Thurzo and K. Gmucova, Phys. Status Solidi A **160**, 89 (1997).
- <sup>23</sup>B.-G. Yoon and C. Lee, J. Appl. Phys. **60**, 673 (1986).
- <sup>24</sup>R. E. Hummel, *Electronic Properties of Materials* (Springer, Berlin, 1992).
- <sup>25</sup>K. Herz and M. Powalla, Appl. Surf. Sci. **91**, 87 (1995).
- <sup>26</sup>R. D. McGraph, J. Doty, G. Lupino, G. Ricker, and J. Vallerga, IEEE Trans. Electron Devices **34**, 2555 (1987).
- <sup>27</sup>W. C. McColgin, J. P. Lavine, J. Kyan, D. N. Nichols, and C. V. Stancampiano, International Electron Device Meeting, 13–16 December 1992, p. 113.